Intraorgan Biodistribution and Dosimetry of ^{153}Sm-Ethylenediaminetetramethylene Phosphonate in Juvenile Rabbit Tibia: Implications for Targeted Radiotherapy of Osteosarcoma

Stephanie C. Essman, DVM[1]; Michael R. Lewis, PhD[1–3]; and William H. Miller, PhD[3]

[1]Department of Veterinary Medicine and Surgery, University of Missouri-Columbia, Columbia, Missouri; [2]Department of Radiology, University of Missouri-Columbia, Columbia, Missouri; and [3]Nuclear Science and Engineering Institute, University of Missouri-Columbia, Columbia, Missouri

Targeted radiotherapy using ^{153}Sm-ethylenediaminetetramethylene phosphonate (^{153}Sm-EDTMP) is currently under investigation for treatment of primary osteosarcoma. Human osteosarcoma most frequently occurs in skeletally immature individuals, and previous studies in a juvenile rabbit model demonstrated that clinically significant damage to developing physeal cartilage might occur as a result of systemic ^{153}Sm-EDTMP therapy. The aim of this study was to determine the distribution of ^{153}Sm-EDTMP within the tibias of juvenile rabbits and estimate the radiation-absorbed doses delivered to the physeal cartilage. **Methods:** Eight-week-old New Zealand White rabbits were injected intravenously with 7.57 kBq (280 μCi) of ^{153}Sm-EDTMP. At 21 h after injection, the biodistribution of ^{153}Sm in the epiphysis, metaphysis, diaphysis, and red marrow of the tibia was obtained. Two-dimensional digital autoradiography was performed on 2-mm sections of tibias for qualitative comparison with the biodistribution data. Self-tissue and cross-tissue absorbed doses were calculated using absorbed fractions generated by the Monte Carlo particle transport code MCNP-4C. **Results:** The highest uptakes (percentage injected dose per gram [%ID/g] of tissue) of ^{153}Sm, 1.99–2.56 %ID/g, were found in the proximal and distal metaphyses, 70%–73% of which localized within 3 mm of the physeal cartilage. The second highest tissues of uptake were the proximal and distal epiphyses, at 0.33–0.62 %ID/g. Digital autoradiography imaging confirmed that the majority of ^{153}Sm deposited in the tibia localized to these tissues. Radiation-absorbed doses to the proximal and distal metaphyses were 183 and 130 mGy/MBq, respectively, and those to the proximal and distal epiphyses were 141 and 43.4 mGy/MBq, respectively. These tissues represented the only source compartments contributing to the physeal cartilage doses of 50.0 mGy/MBq for the proximal physis and 39.2 mGy/MBq for the distal physis. **Conclusion:** The ^{153}Sm absorbed doses to the physeal cartilage were consistent with values that can cause dose-limiting damage to rapidly proliferating and differentiating chondrocytes. The pronounced uptake in the juvenile epiphysis indicates that the proliferating zone of the physis can be irradiated from multiple areas, which could increase the expression and degree of radiation damage. Further investigation of the effects of ^{153}Sm-EDTMP on immature physeal cartilage is warranted to develop optimized treatment regimens.

Key Words: ^{153}Sm-ethylenediaminetetramethylene phosphonate; osteosarcoma; physeal cartilage; absorbed dose

J Nucl Med 2005; 46:2076–2082

Radionuclide therapy is often used for palliation of bone pain secondary to metastases of breast, prostate, and lung cancer. $^{89}SrCl_2$ and ^{153}Sm-ethylenediaminetetramethylene phosphonate (^{153}Sm-EDTMP) have been approved by the Food and Drug Administration for palliation of bone pain secondary to metastases. These treatments have proven safe and efficacious at a dose of 37 MBq/kg (1 mCi/kg) (*1–5*). Studies in dogs and limited clinical studies in humans have suggested that intravenous radionuclide therapy using ^{153}Sm-EDTMP can be an effective component of a multimodality treatment regimen for primary bone tumors (*6–10*), at doses as high as 1,110 MBq/kg (30 mCi/kg) with stem cell rescue (*10*). Primary bone tumors tend to be radioresistant, and the dose of external beam radiation that is needed to achieve a tumoricidal dose would result in severe radiation injury to surrounding tissues. Therefore, by using a bone-seeking radiopharmaceutical, such as ^{153}Sm-EDTMP, in combination with external beam radiation, the overall dose to the tumor can be increased substantially, sparing the normal surrounding tissues. Expansion of these studies has lead to the use of this agent in clinical trials for juvenile osteosarcoma.

Received May 4, 2005; revision accepted Aug. 17, 2005.

For correspondence or reprints contact: Stephanie C. Essman, DVM, Department of Veterinary Medicine and Surgery, College of Veterinary Medicine, University of Missouri-Columbia, 379 E. Campus Dr., Columbia, MO 65211.
E-mail: essmans@missouri.edu

^{153}Sm-EDTMP possesses physical properties that make it an optimal therapeutic radiopharmaceutical for treatment of bone cancers. The medium-energy β^--particles (E_{max} = 0.640 MeV at 30%, 0.710 MeV at 50%, 0.810 MeV at 20%) limit the deposition of ionizing radiation to a distance of approximately 3 mm from the point of decay (*6*). The physical half-life is approximately 1.95 d (46.3 h). ^{153}Sm-EDTMP also emits a 103-keV γ-photon at 28%, which allows imaging of skeletal localization with conventional γ-cameras (*1,6*). Upon intravenous injection, ^{153}Sm-EDTMP localizes in areas of increased osteoblastic activity, and deposition of this complex is directly correlated with matrix formation. This can occur in regions of bone growth and remodeling and in tumor formation (*1,6*). Chelation of ^{153}Sm to EDTMP is advantageous because it enhances skeletal uptake of ^{153}Sm while markedly limiting its deposition in soft tissues.

The effects of external beam radiation on growing physeal cartilage have been established (*11–16*), but the effects of ^{153}Sm-EDTMP on physeal development and growth plate closure have not been evaluated until recently (*17*). Because children are most commonly afflicted with the primary bone cancer osteosarcoma, insults to the immature physes administered by sources of ionizing radiation could cause permanent cessation of growth or growth deformities and possibly predispose these patients to pathologic fractures. Because ^{153}Sm-EDTMP localizes in areas of high osteoblastic activity, such as the zone of provisional calcification, substantial injury to physeal cartilage in immature normal bone can occur. In a previously published study (*17*), we determined the effects of ^{153}Sm-EDTMP on the development of long bone physes in a juvenile rabbit model and have correlated these findings to radiographic and histopathologic physeal cartilage damage. Our data suggested that clinically significant damage to the developing physeal cartilage might occur as the result of intravenous administration of ^{153}Sm-EDTMP. In these juvenile rabbits, proliferating chondrocytes were exposed to ionizing radiation emitted from ^{153}Sm-EDTMP localized in the periphyseal bone. This collateral damage resulted in significant alterations in radial bone length. Profound disturbances in physeal area and morphology, as well as in synthetic behavior of physeal chondrocytes, were found not only in the radius but also in the tibia and humerus. The consistent and widespread disturbances to the developing physeal tissues have immediate clinical implications for the use of ^{153}Sm-EDTMP in the treatment of juvenile osteosarcoma.

Our initial study (*17*) did not quantify the radiation-absorbed doses that were delivered to the physes. In previous work with external beam radiation using photons, it has been determined that the dose–effect relationship of cartilage is steep between doses of 15 and 30 Gy, with the saturation dose occurring at levels of 25–40 Gy (*11,16*). The goal of this study was to determine the intraorgan deposition and dosimetry of ^{153}Sm-EDTMP in bone and physeal cartilage in the juvenile rabbit model. These factors may have important implications for osteosarcoma therapy and toxicity.

MATERIALS AND METHODS

Biodistribution Studies

This animal experiment was conducted in compliance with the regulations of the Animal Care and Use Committee of the University of Missouri-Columbia. Five juvenile (8-wk-old) male New Zealand White rabbits (Myrtle Rabbit Tree) weighing approximately 2 kg (range, 2.04–2.19 kg; mean, 2.10 kg) were used. A dose of 7.57 kBq (280 μCi) of ^{153}Sm-EDTMP was injected intravenously via an ear vein catheter, and animals were sacrificed 21 h after administration. The tibias were dissected from the remainder of the skeleton and all soft tissues were completely removed to ensure no extraneous contamination occurred. Bone tissues collected from the tibias by sharp dissection included proximal and distal epiphysis, proximal and distal physis, proximal and distal metaphysis, diaphysis, and red marrow. In the metaphyses, the majority of radioactivity was deposited within 3 mm of the physes. Therefore, the metaphyses were each divided into 2 sections: proximal and distal metaphysis 1 (3-mm section immediately adjacent to the physis) and proximal and distal metaphysis 2 (remainder of tissue.) Tissues were weighed and counted in an automated γ-counter with an empty vial and a standard of the injected dose, such that the background- and decay-corrected values were calculated as percentage injected dose per gram of tissue (%ID/g) and %ID per tissue (%ID/tissue). The injected doses and the standard of the injected dose were weighed with an accuracy of >99%. The amount of radioactivity in each injected dose was then calculated by multiplying the background-corrected value for the standard by the ratio of the weight of the injected dose divided by the weight of the standard.

Physeal cartilage was contaminated with a small amount of metaphyseal tissue. Therefore, physeal contamination was reassigned to the metaphysis 1 compartment. It was assumed that no uptake of ^{153}Sm-EDTMP occurred in the physis, because vasculature termination occurs adjacent to the proliferating cartilage (*18*), and ^{153}Sm-EDTMP remains fixed in the extracellular matrix after deposition (*19*).

Digital Autoradiography

Two-dimensional digital autoradiography was performed in corresponding 2-mm sections of contralateral tibias (n = 5) to image the intraorgan distribution of radioactivity (Fig. 1). Autoradiograms were acquired using a Bioscan AR-2000 scanner equipped with a 4-mm collimator with a 10 × 200 mm field of view and WinScan 2D, version 3.00, software (Bioscan). Increments of 2 mm and a 2-min acquisition per lane were used, for a total of 24 lanes per tibial section. Lane overlap correction was automatically performed by WinScan 2D.

Bone Tissue Dosimetry

Bone tissue radiation-absorbed doses were calculated using the Monte Carlo radiation transport code MCNP-4C (*20*). A right cylinder model of the tibia was generated from measurements of radiographs to approximate compartment radii and volumes (Fig. 2). Tissue volumes calculated from right cylinder geometries were within 0.2% of the values measured by radiography. Red marrow was assumed to be equivalent to water having a density of 0.979 g/cm^3, approximating that of whole blood. Physeal cartilage was assumed to have unit density. The epiphyses, diaphysis, and me-

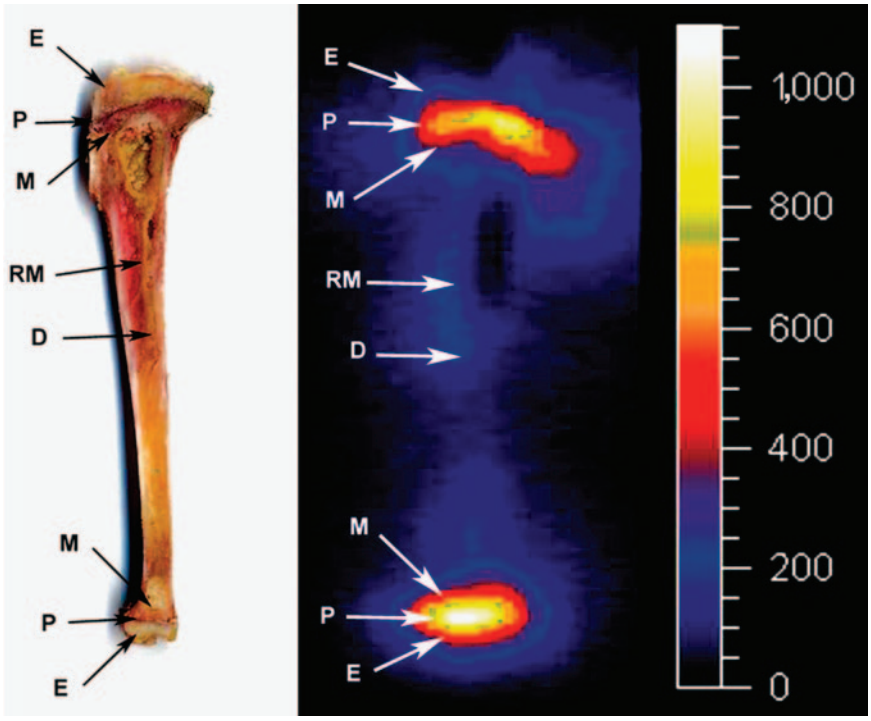

FIGURE 1. Representative digital autoradiogram (middle) of ^{153}Sm deposition in tibia of 8-wk-old male New Zealand White rabbit. (Right) False color scale of radioactivity concentration. (Left) Image of corresponding bone section, indicating locations of epiphysis (E), physis (P), metaphysis (M), red marrow (RM), and diaphysis (D).

taphyses were modeled with a combination of water and 27% (by weight) calcium with a density of 1.37 g/cm^3. Tissue of unit density was assumed to surround the bone.

β-Particles, induced bremsstrahlung radiation, and the 103-keV primary photons from the decay of ^{153}Sm were included in the modeling using the photon electron mode of MCNP. To appropriately account for the β-energies resulting from the decay of ^{153}Sm, the NUCDECAY code (*21*) was used to generate the β-emission spectrum. For each β-energy in the spectrum generated by NUCDECAY, an MCNP calculation was performed for this monoen-

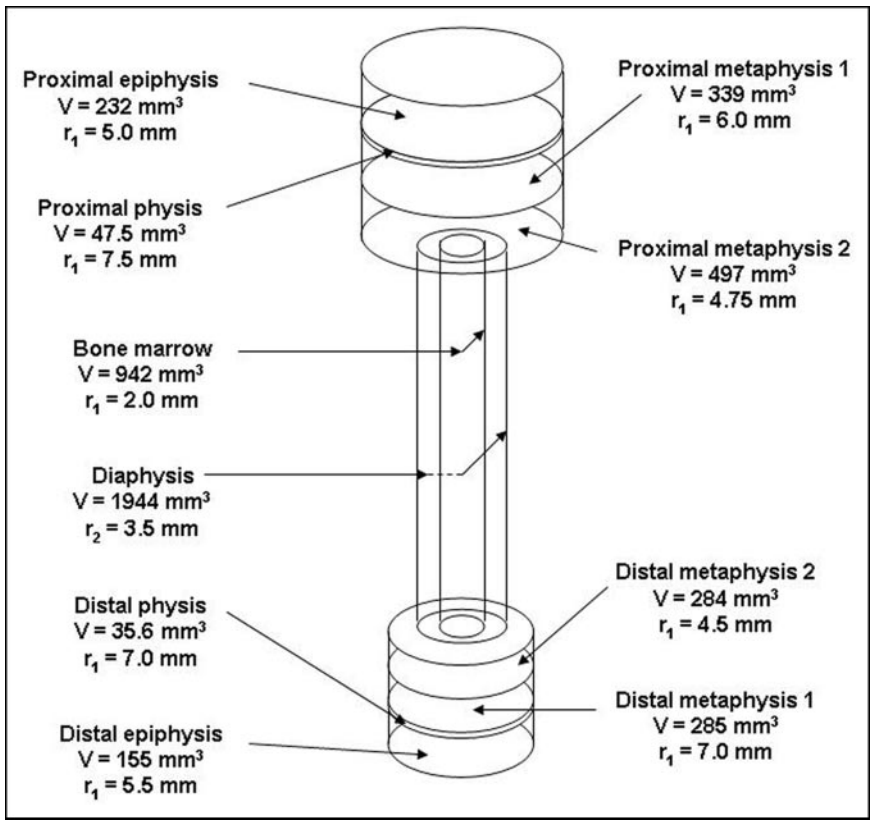

FIGURE 2. Right cylinder model of tibia generated from radiographic measurements shows approximate radii (r_1 = radius of filled cylinder; r_2 = outside radius of hollow cylinder) and volumes of different compartments evaluated.

ergetic electron. The resulting absorbed fractions in all regions of the problem were subsequently numerically integrated over the ^{153}Sm spectra. For each monoenergetic β-energy, 5×10^4 histories were run on a standard desktop personal computer, resulting in absorbed energy uncertainties of no more that 1% for each electron energy. When these absorbed fractions were averaged over the 108 energy bins representing a β-spectrum, the final uncertainties were much less than 1%. Standard energy cutoffs (0.001 MeV) and weight cutoffs for both β-particles and photons were used.

On the basis of the results of previously published studies (*22*), uptake of ^{153}Sm was assumed to occur in a linear manner over the first 15 min after administration, and physical decay was invoked thereafter. Radioactivity was assumed to be uniformly distributed throughout the bone compartments, except in the metaphyses, which was divided into 2 regions of uniform uptake as discussed. Self-absorbed and cross-tissue radiation energy was determined as the amount of absorbed energy in each bone compartment per radioactive decay. This approach assumed that tibias of similar size in different animals had similar uptake characteristics, and the resulting absorbed doses represented an average of that absorbed by each tibial tissue.

RESULTS

The animals were sacrificed and tissues were collected at 21 h after injection. This time point was chosen because it was sufficiently long to allow for maximum uptake of radioactivity in the bone and clearance from the nonosseous tissues. The highest uptakes of ^{153}Sm-EDTMP in the juvenile rabbit tibia were the proximal and distal metaphyses, at 2.56 %ID/g and 1.99 %ID/g, respectively. In the proximal metaphysis, an average of 73.1% of the tissue radioactivity, in %ID/tissue, was found in the 3-mm section immediately adjacent to the physis (metaphysis 1), and an average of 26.9% was found in the remainder of the tissue (metaphysis 2). In the distal metaphysis, on average, 70.1% of the tissue's radioactivity was localized to the metaphysis 1 compartment, whereas an average of 29.9% deposited in the remainder of the tissue (metaphysis 2).

The second highest uptakes were observed in the proximal (0.62 %ID/g) and distal (0.33 %ID/g) epiphyses. Uptake in the diaphysis, the largest tissue, was 0.27 %ID/g, whereas red marrow uptake was negligible (0.02 %ID/g). Because previous studies have shown that termination of the vasculature required for delivery of ^{153}Sm-EDTMP occurs before the zone of proliferating chondrocytes (*18*), uptake in the physes was assumed to be zero.

Digital autoradiography of 2-mm sections of the contralateral tibias confirmed the distribution of ^{153}Sm-EDTMP in the various bone compartments 21 h after injection. A representative autoradiogram is shown in Figure 1. The highest concentrations of radioactivity localized to periphyseal bone, predominantly within the metaphysis 1 and epiphysis areas. Localization in the diaphysis and marrow occurred to a much lesser degree. Digital autoradiography analysis correlated qualitatively with the intratibial biodistribution of ^{153}Sm-EDTMP determined by tissue dissection and radiation counting (*23*).

Although intraorgan biodistribution was obtained at a single time point in the juvenile rabbit tibia, Goeckeler et al. (*22*) showed that femoral uptake of ^{153}Sm-EDTMP in rats was not significantly different from 15 min to 72 h after injection. Therefore, accumulation of ^{153}Sm-EDTMP in juvenile rabbit tibia was assumed to occur in a linear manner over the first 15 min after administration, after which physical decay was invoked. At most, this assumption represented 0.5% of the radiation-absorbed dose delivered to the juvenile rabbit tibia during the 15-min uptake period.

Using the intraorgan biodistribution data in %ID/tissue (Table 1) and the results of the MCNP calculations of absorbed energy per decay, the radiation-absorbed doses to the tibial tissues were estimated using a right cylinder model of the juvenile rabbit tibia (Fig. 2). The results of these dosimetry calculations are given in Table 2. For an injected dose of 37 MBq/kg (1 mCi/kg), the highest radiation-absorbed doses were delivered to the metaphyses (4.81–7.18 Gy) and epiphyses (1.61–5.22 Gy). Self-doses accounted for 94.0%–98.4% of the total in these tissues, 99.9%–100% of which were attributable to β^--radiation. The absorbed doses delivered to the proximal and distal physes from all bone tissues were estimated at 1.85 and 1.45 Gy, respectively, for an injected dose of 37 MBq (1 mCi) in a 1-kg juvenile rabbit. These doses resulted entirely from β^--irradiation from the metaphysis 1 and epiphysis compartments. In the proximal physis, 61.0% of the absorbed dose originated from the proximal metaphysis 1, and 39.0% arose from the epiphysis. The distal metaphysis 1 accounted for 77.0% of the cross-tissue dose to the distal physis, whereas the distal epiphysis accounted for the remaining 23.0%.

DISCUSSION

Differences in radiation sensitivity are attributed to the rate of replication inherent to the critical cells in the treated or irradiated tissue; therefore, ionizing radiation affects all

TABLE 1
Intraorgan Biodistribution (n = 5) of ^{153}Sm-EDTMP in Tibias of 8-Week-Old Male New Zealand White Rabbits at 21 Hours After Injection

Tissue	%ID/g	%ID/tissue
Proximal epiphysis	0.62 ± 0.16	0.59 ± 0.21
Proximal metaphysis 1	2.15 ± 0.59	0.87 ± 0.16
Proximal metaphysis 2	0.41 ± 0.08	0.32 ± 0.05
Diaphysis	0.27 ± 0.03	0.62 ± 0.05
Red marrow	0.02 ± 0.00	0.02 ± 0.00
Distal metaphysis 1	1.40 ± 0.11	0.47 ± 0.06
Distal metaphysis 2	0.59 ± 0.05	0.20 ± 0.03
Distal epiphysis	0.33 ± 0.04	0.12 ± 0.04

Metaphysis 1 compartment = 3 mm of tissue directly adjacent to physis, corresponding to maximum range of ^{153}Sm β-particle in hard tissue; metaphysis 2 = remainder of tissue. Values are given as mean ± SD.

TABLE 2
Radiation-Absorbed Dose Estimates from ^{153}Sm-EDTMP in Tibias of 8-Week-Old Male New Zealand White Rabbits

Tissue	mGy/MBq (rad/mCi)
Proximal epiphysis	141 (522)
Proximal physis	50.0 (185)
Proximal metaphysis 1	144 (534)
Proximal metaphysis 2	39.4 (146)
Diaphysis	17.4 (64.5)
Red marrow	5.38 (19.9)
Distal metaphysis 1	88.2 (327)
Distal metaphysis 2	42.0 (155)
Distal physis	39.2 (145)
Distal epiphysis	43.4 (161)

Metaphysis 1 compartment = 3 mm of tissue directly adjacent to physis, corresponding to maximum range of ^{153}Sm β-particle in hard tissue; metaphysis 2 = remainder of tissue.

phases of physeal activity, but especially chondrocytes and small blood vessels (*11,14,24*). Chondrocytes in the zone of proliferation in physeal cartilage are rapidly dividing, and considered differentiating intermitotic cells, and thereby radiosensitive (*25*). In addition, the metaphyseal vasculature is lined with endothelium. Radiation damage to these blood vessels results in irregular production of osteoid and faulty bone formation (*14*). Damage to the proliferating chondrocytes leads to a disruption of the anisotropic environment of the cartilage (*11*) and metaphyseal vascular injury results in deficient absorptive processes, each contributing to growth disturbances. In our initial study (*17*), radiation damage was expressed as an irregular arrangement of the normal columnar appearance to the physeal chondrocytes, absolute shortening of bone length, and decreased expression of cell markers that are seen in normal endochondral ossification.

In the current study, there was high radiopharmaceutical uptake in the epiphysis as well as in the metaphysis of the bone. The pronounced uptake in the juvenile rabbit epiphysis has important clinical implications, as this finding indicates that the proliferating zone of the physis can be irradiated from multiple areas, possibly increasing the expression and degree of radiation damage. There are 2 reasons for the uptake in the epiphyseal region of the bone. Initially, the structural events at the developing secondary center of ossification in the postnatal period parallel the events at the physis (*18*). The matrix adjacent to the hypertrophic cells mineralizes and the hypertrophic cell lacunae are invaded by vessels of the cartilage canals carrying mesenchymal cells and preosteoblasts (*18*). Because of the osteoblastic activity that occurs in this area during growth, localization of bone-seeking radiopharmaceuticals would occur, resulting in additional physeal irradiation and damage to the proliferating chondrocytes.

In addition, there are 3 major vascular supplies to the growth plate in a rabbit (*18*). The epiphyseal artery enters the secondary center of ossification. The terminal branches of this artery pass through the secondary center of ossification to terminate on the outer surface of the reserve zone of the physis, supplying oxygen and nutrients to the proliferating chondrocytes by diffusion (*18,26*). The reserve zone of cartilage is located just adjacent to the zone of proliferation; however, the reserve zone does not participate in active growth through cell proliferation or matrix synthesis. The second vascular supply is the main nutrient artery, which enters at the level of the mid-diaphysis and bifurcates, sending an arterial branch within the medullary canal toward each metaphysis. The terminal branches are adjacent to the zone of hypertrophy and constitute the metaphyseal blood supply (*18*). Finally, the periphery of the growth plate is supplied by metaphyseal arteries with periosteal arteries providing a collateral supply (*18*). These vessels are lined with endothelium that is radiosensitive; thus, damage to these vessels can result in faulty bone formation. In addition, damage to these vessels can lead to a decrease in oxygen tension and nutritional elements, leading to disruption of longitudinal growth. Comparatively, the organization of the physeal cartilage and vascular distribution are similar in the human skeleton (*18,27,28*); therefore, the same pattern of radiopharmaceutical distribution and uptake would be expected in humans.

In previous work (*17*), epiphyseal uptake was not observed in scintigraphic images of juvenile rabbits receiving ^{153}Sm-EDTMP, likely because of the relative low anatomic resolution of the γ-camera compared with the digital autoradiography system used here. Furthermore, quantitative autoradiography of ^{153}Sm-EDTMP deposition in the femurs and tibias of rats demonstrated high uptake only in the metaphyseal area adjacent to the physis, moderate uptake in trabecular bone, and lower uptake in the epiphysis (*29*). Unlike rabbits and humans, epiphyseal cartilage vessels are not present in rodents (*26*); therefore, differences in bone physiology may give rise to differences in ^{153}Sm-EDTMP deposition between species.

The absolute shortening after irradiation of long bones is one of the sequelae of radiation therapy. Studies evaluating external beam therapy show that restoration of normal columnar arrangement can occur; however, the likelihood and time frame for this to occur depend on the total dose of radiation (*16,24*). These studies have reported that the dose–effect relationship may be particularly steep between the doses of 15 and 30 Gy, with the saturation dose occurring at levels of 25–40 Gy (*11,16*). In a study evaluating the dose–effect relationship as a function of age, it was noted that when the parameter used for estimating the radiation effect was the overall shortening of the irradiated limb, greater effects were seen in less mature bones. However, when growth remaining after irradiation was considered, the age at the time of irradiation did not influence the final effect, but the total dose of irradiation was the most important factor (*16*). In our initial study (*17*), a significant shortening of the radius in rabbits treated with ^{153}Sm-

EDTMP was observed compared with that of control animals. Although shortening was only observed in the radius, profound radiation damage to the physes was also detected in the humerus and tibia. However, one limitation of that study was a duration of only 8 wk, at which time the physes in humerus and tibia may not have reached maturity, precluding evaluation of shortening or deformity in those bones. An additional limitation of that study was a lack of quantification of the total ^{153}Sm-EDTMP absorbed dose delivered to the physeal cartilage.

In the current study, the radiation-absorbed doses delivered to the physes from all bone tissues were estimated at 1.45–1.85 Gy for an injected dose of 37 MBq (1 mCi) in a 1-kg juvenile rabbit. This value was consistent with that which can cause dose-limiting radiopharmaceutical damage to rapidly proliferating and differentiating cells, such as bone marrow stem cells (*30*). It was not surprising that this absorbed dose resulted in profound damage to developing physeal cartilage in the juvenile tibia found in our previous study (*17*). It remains to be determined whether this damage is reversible or dose limiting to the physeal cartilage. However, it should be noted that the radiation-absorbed dose was deposited slowly over a short range from an internal emitter, and the dose–effect relationship of ^{153}Sm-EDTMP on physeal cartilage cannot be compared directly to that arising from external beam irradiation. Surprisingly, the current study showed that there was high radiopharmaceutical uptake in the epiphysis as well as in the metaphysis. Thus, the use of high-dose ^{153}Sm-EDTMP for the treatment of juvenile osteosarcoma will likely deliver considerably higher absorbed doses to the physes and may result in increased expression and degree of radiation damage arising from multiple source tissues. In addition, the biodistribution of ^{153}Sm-EDTMP may be altered within a skeletal site with tumor, resulting in considerably higher uptake and absorbed dose delivered to the tumor and surrounding bone tissues. Previous studies have shown that a tumor burden can result in an increase in absolute uptake by a factor of 5, with a concomitant increase in dose dependency on the tumor and healthy bone tissues (*3*). At this time, there are no established protocols for development of an orthotopic rabbit model of skeletal osteosarcoma. However, the effects of tumor burden could be evaluated further using a rabbit drill hole model (*31*), which mimics the presence of an osteoblastic lesion. An additional objective of future studies will be to evaluate strategies to minimize permanent physeal cartilage damage from ^{153}Sm-EDTMP in the juvenile rabbit model, with the goal of developing optimized treatment regimens for human clinical trials.

CONCLUSION

This rabbit biodistribution study allowed quantification of the distribution of radioactivity in bone compartments after injection of ^{153}Sm-EDTMP and determination of the radiation dose delivered to the physis from all tissues within the bone. The absorbed dose of 1.45–1.85 Gy for an injected dose of 37 MBq/kg (1 mCi/kg) is enough to cause dose-limiting radiopharmaceutical damage to rapidly proliferating and differentiating cells, such as immature chondrocytes, possibly leading to growth disturbances. The use of high-dose ^{153}Sm-EDTMP for the treatment of juvenile osteosarcoma may result in increased expression and degree of radiation damage arising from multiple source tissues. The average thickness of the proximal tibial physis in humans 5–17 y of age is 1.51 ± 0.27 mm (*32*), compared with approximately 1 mm in 8-wk-old male New Zealand White rabbits. Given that the maximum range of ^{153}Sm β^--emissions is approximately 3 mm in hard tissue, similar intraorgan deposition may give rise to comparable absorbed doses to tibial physes in children and adolescents. However, definitive extrapolations of physeal cartilage radiation-absorbed doses from juvenile rabbits to humans are not trivial. Such extrapolations will require that extensive comparative studies in osteosarcoma patients demonstrate minimal and predictable differences between the 2 species. Nonetheless, future studies are warranted to evaluate strategies for minimizing permanent physeal cartilage damage from ^{153}Sm-EDTMP in the juvenile rabbit model, with the goal of developing optimized treatment regimens for human clinical trials. However, in the context of high-dose therapy, further investigation of the effects of ^{153}Sm-EDTMP on immature physeal cartilage is needed to develop optimized treatment regimens.

ACKNOWLEDGMENTS

The authors thank Darren Loula and Serena Carter for excellent technical support as well as Steve Stein and Bioscan (Washington, D.C.) for helpful discussions on 2-dimensional digital autoradiography. We also acknowledge the U.S. Department of Veterans Affairs, for providing the use of facilities and resources at the Harry S. Truman Memorial Veterans' Hospital in Columbia, MO.

REFERENCES

1. Rodriguez V, Betcher D. ^{153}Sm-EDTMP. *J Pediatr Oncol Nurs.* 1998;15:95–97.
2. Holmes RA. [^{153}Sm]EDTMP: a potential therapy for bone cancer pain. *Semin Nucl Med.* 1992;22:41–45.
3. Turner JH, Martindale AA, Sorby P, et al. Samarium-153 EDTMP therapy of disseminated skeletal metastasis. *Eur J Nucl Med.* 1989;15:784–795.
4. Serafini AN, Houston SJ, Resche I, et al. Palliation of pain associated with metastatic bone cancer using samarium-153 lexidronam: a double-blind placebo-controlled clinical trial. *J Clin Oncol.* 1998;16:1574–1581.
5. Bayouth JE, Macey DJ, Kasi LP, Fossella FV. Dosimetry and toxicity of samarium-153-EDTMP administered for bone pain due to skeletal metastases. *J Nucl Med.* 1994;35:63–69.
6. Lattimer JC, Corwin LA, Stapleton J, et al. Clinical and clinicopathologic response of canine bone tumor patients to treatment with samarium-153-EDTMP. *J Nucl Med.* 1990;31:1316–1325.
7. Franzius C, Bielack S, Vollet B, Jurgens H, Schober O. High-activity samarium-153-EDTMP therapy in unresectable osteosarcoma. *Nuklearmedizin.* 1999;38:337–340.
8. Franzius C, Bielack S, Flege S, Eckardt J, Sciuk J, Schober O. High-activity samarium-153-EDTMP therapy followed by autologous peripheral blood stem cell support in unresectable osteosarcoma. *Nuklearmedizin.* 2001;40:215–220.
9. Moe L, Boysen M, Aas M, Lonaas L, Gamle H, Bruland OS. Maxillectomy and

targeted radionuclide therapy with ^{153}Sm-EDTMP in recurrent canine osteosarcoma. *J Small Anim Pract.* 1996;37:241–246.
10. Anderson PM, Wiseman GA, Dispenzieri A, et al. High dose samarium-153 ethylene diamine tetramethylene phosphonate: low toxicity of skeletal irradiation in patients with osteosarcoma and bone metastases. *J Clin Oncol.* 2001;20:189–196.
11. Eifel PJ, Donaldson SS, Thomas PF. Response of growing bone to irradiation: a proposed late effects scoring system. *Int J Radiat Oncol Biol Phys.* 1995;31:1301–1307.
12. Melanotte PL, Follis RH. Early effects of x-irradiation on cartilage and bone. *Am J Pathol.* 1961;39:1–7.
13. Rutherford H, Dodd GD. Complications of radiation therapy: growing bone. *Semin Roentgenol.* 1974;7:15–26.
14. Probert JC, Parker BR. The effects of radiation therapy on bone growth. *Radiology.* 1975;114:155–162.
15. Parker RG, Berry HC. Late effects of therapeutic irradiation on the skeleton and bone marrow. *Cancer.* 1976;37:1162–1171.
16. Gonzalez DG, Breur K. Clinical data from irradiated growing long bones in children. *Int J Radiat Oncol Biol Phys.* 1983;9:841–846.
17. Essman SC, Lattimer JC, Cook JL, Turnquist S, Kuroki K. Effects of ^{153}Sm-EDTMP on physeal and articular cartilage in juvenile rabbits. *J Nucl Med.* 2003;44:1510–1515.
18. Rivas R, Shapiro F. Structural states in the development of the long bones and epiphyses: a study in the New Zealand White rabbit. *J Bone Joint Surg Am.* 2002;84:85–100.
19. Heggie JCP. Radiation absorbed dose calculations for samarium-153-EDTMP localized in bone. *J Nucl Med.* 1991;32:840–844.
20. Briesmeister JE. *MCNP: A general Monte Carlo N-Particle Transport Code, version 4C*. Report LA-13709-M. Los Alamos, NM: Los Alamos National Laboratory; 2000.
21. ORNL. *NUCDECAY: Nuclear Decay Data for Radiation Dosimetry Calculations for ICRP and MIRD*. RSICC Data Library DLC-172. Oak Ridge, TN: Oak Ridge National Laboratory; 1995.
22. Goeckeler WF, Edwards B, Volkert WA, Holmes RA, Simon J, Wilson D. Skeletal localization of samarium-153 chelates: potential therapeutic bone agents. *J Nucl Med.* 1987;28:495–504.
23. Lewis MR, Zhang J, Jia F, et al. Biological comparison of ^{149}Pm-, ^{166}Ho-, and ^{177}Lu-DOTA-biotin pretargeted by CC49 scFv-streptavidin fusion protein in xenograft-bearing nude mice. *Nucl Med Biol.* 2004;31:213–223.
24. Frantz CH. Extreme retardation of epiphyseal growth from roentgen irradiation. *Radiology.* 1950;55:720–724.
25. Gonzalez DG, Van Dijk DP. Experimental studies on the response of growing bones to x ray and neutron irradiation. *Int J Radiat Oncol Biol Phys.* 1983;9:671–677.
26. Shapiro F. Epiphyseal and physeal cartilage vascularization: a light microscopic and tritiated thymidine autoradiographic study of cartilage canals in newborn and young postnatal rabbit bone. *Anat Rec.* 1998;252:140–148.
27. Shim SS, Leung G. Blood supply of the knee joint: a microangiographic study in children and adults. *Clin Orthop.* 1986;208:199–125.
28. Ballock RT, O'Keefe RJ. Physiology and pathophysiology of the growth plate. *Birth Defects Res Part C Embryo Today.* 2003;69:123–143.
29. Ghiron J, Volkert WA, Garlich J, Holmes RA. Determination of lesion to normal bone uptake ratios of skeletal radiopharmaceuticals by QARG. *Nucl Med Biol.* 1991;18:235–240.
30. Goldenberg DM. Advancing role of radiolabeled antibodies in the therapy of cancer. *Cancer Immunol Immunother.* 2003;52:281–296.
31. Subramanian G, McAfee JG, Thomas FD, Feld TA, Zapf-Longo C, Palladino E. New diphosphonate compounds for skeletal imaging: comparison with methylene diphosphonate. *Radiology.* 1983;149:823–828.
32. Dardzinski BJ, Laor T, Schmithorst VJ, Klosterman L, Graham TB. Mapping T2 relaxation time in the pediatric knee: feasibility with a clinical 1.5-T MR imaging system. *Radiology.* 2002;225:233–239.